Electrical conductivity structure of the Purcell Anticlinorium in southeast British Columbia and northwest Montana[1]

Jagdish C. Gupta and Alan G. Jones

Abstract: Magnetotelluric data from almost 200 sites were acquired by a commercial contractor over the Precambrian Purcell Anticlinorium west of the Rocky Mountains of Canada and the United States. Fifteen east–west profiles cross the anticlinorium between latitudes of 48 and 49.5°N, and provide a grid suitable for a regional three-dimensional study of the electrical structure of predominantly the upper crust. The data show essentially a resistive uppermost crust, varying from 2 to 6 km in thickness, over a strongly conductive widespread electrical "basement." The general electrical strike of this conductive basement is found to be N30°W, which concurs with the surface geological trend of the region. The data from all profiles were inverted one dimensionally, and from two of the profiles two dimensionally, using different algorithms, to test the accuracy of the one-dimensional images. The main features found are (*i*) the sediments in the Upper and Middle Belt–Purcell strata are, in general, more conducting than those in the Lower Belt strata of the anticlinorium; (*ii*) the basement conductor appears to be strongest just to the south of the Canada – United States border, with resistivities of around 1 $\Omega \cdot$ m or less; (*iii*) the western part of the region is more conducting than the eastern part, suggesting that the sources of sedimentation on the two sides of the region were different; (*iv*) the enhanced conductivity observed can be explained by the presence of mineralization (copper, etc.), rather than other geophysical causes; (*v*) near the western edge of the Rocky Mountain trench the conductivity increases downwards from near the surface, and near the eastern edge it increases downwards from a depth of about 2 km, suggesting the presence of the asymmetric mineralization in it; (*vi*) a few kilometres west of the Rocky Mountain trench in the resistive terrain there exist two narrow, vertical, and significantly conductive electrical "conduits"; and (*vii*) the pervasive conductive basement extends farther east and north than the present location of the copper sulphide mines in northwestern Montana.

Résumé : Un levé magnétotellurique, réalisé par un exécutant commercial, a procuré des données portant sur près de 200 sites localisés à l'intérieur de l'anticlinorium de Purcell précambrien, à l'ouest des Rocheuses du Canada et des États-Unis. Quinze lignes de profils orientées est–ouest traversent l'anticlinorium entre les latitudes de 48 et 49,5°N, et les données obtenues à l'intérieur de ce quadrillage sont suffisantes pour permettre une étude régionale en trois dimensions de la structure du champ électromagnétique surtout de la croûte supérieure. Les données indiquent une croûte supérieure essentiellement résistive, variant en épaisseur de 2 à 6 km, reposant sur un « socle » électromagnétique étendu à forte conductivité. La direction électromagnétique générale de ce socle conducteur est établie à N30°W, coïncidant avec la direction en surface de la structure géologique de la région. Sur une base unidimensionnelle, les données de tous les profils étaient inversées, et c'est également vrai pour deux de ces profils calculés avec deux dimensions; on a utilisé différents algorithmes pour tester la précision que procurent les images unidimensionnelles. Les principales caractéristiques mises en évidence sont (*i*) les sédiments des strates de l'Assemblage de Belt–Purcell supérieur et médian forment, en général, un meilleur conducteur que les sédiments des strates de l'Assemblage inférieur de l'anticlinorium; (*ii*) le substratum se comporte comme un conducteur plus intense dans la région juste au sud de la frontière Canada–États-Unis, avec des résistivités autour de 1 $\Omega \cdot$ m ou moins; (*iii*) on observe que la partie occidentale de la région étudiée est plus conductrice que sa partie orientale, ce qui suggère que les sources de sédiment des deux côtés de la région étaient différentes; (*iv*) le rehaussement de la conductivité observé peut être expliqué par la présence de minéraux métalliques (cuivre, etc.), et non par des causes géophysiques; (*v*) près de la bordure occidentale du sillon des Rocheuses, la conductivité augmente avec la profondeur en commençant près de la surface, tandis qu'au voisinage de la bordure

Received December 9, 1994. Accepted March 22, 1995.

J.C. Gupta and A.G. Jones.[2] Geological Survey of Canada, 1 Observatory Crescent, Ottawa, ON K1A 0Y3, Canada.

[1] Geological Survey of Canada Contribution 51594.

[2] Corresponding author (e-mail: jones@cg.emr.ca).

orientale, elle augmente avec la profondeur seulement à partir d'environ 2 km sous la surface, ce qui suggère l'incorporation d'une minéralisation asymétrique; (*vi*) à quelques kilomètres à l'ouest du sillon des Rocheuses, dans le terrain résistif, il existe deux « conduits » électromagnétiques formant des conducteurs étroits et verticaux; et (*vii*) le substratum conducteur persistant se prolonge plus loin à l'est et au nord des sites actuels des mines de sulfures de cuivre dans le nord-ouest du Montana.
[Traduit par la rédaction]

Introduction

The crust of the Cordilleran region of North America is characterized for the most part by high electrical conductivity and high heat flow, and is thin compared with older regions. Jones et al. (1992) and Marquis et al. (1995) have shown that the Omineca Belt (Omineca Crystalline Belt) has a highly conducting lower crust, with resistivities less than 10 $\Omega \cdot$ m (conductivities greater than 0.1 S/m). In contrast, the crystalline crust of cratonic North America is resistive ($>1000\ \Omega \cdot$ m), but is host to a number of significant conductivity anomalies. The transition between these two regions is the Foreland Belt of the Cordillera (Fig. 1). The Foreland Belt consists mainly of para-autochthonous Precambrian and Palaeozoic sedimentary rocks, derived from a long-lived miogeocline that existed on the western border of cratonic North America, lying above a thin sheet of Palaeozoic rocks and gently westward-dipping North American basement (Yoos et al. 1991).

The study area lies in southeastern British Columbia (Canada) and northwestern Montana (U.S.A.) between latitudes 48.0 and 49.5°N and longitudes 114.5 and 116.25°W (Fig. 1). This region was the scene of some of the earliest oil and gas exploration in western North America. Continued accumulation of geological, geochemical, and geophysical data was also stimulated by the search for copper deposits and, more recently, for possibly gas-bearing Palaeozoic sediments overthrust by Precambrian rocks. As part of these activities, regionally extensive magnetotelluric (MT) measurements were made by a commercial contractor during the mid-1980's across the Purcell Anticlinorium in both Canada and the United States.

Our objective is to determine the regional electrical conductivity structure from these MT data, using advanced processing and inversion techniques not available earlier, to supplement the existing knowledge of the underlying crust obtained from geological mapping, drilling activities, and seismic and gravity surveys. The results also provide an opportunity to understand the pervasive mineralization that is present in this region.

The MT data are initially analyzed to determine the gross regional electrical strike and its lateral and vertical variation. The locations of high-conductivity zones are identified qualitatively using the induction (or "Parkinson") arrows. The data are corrected for local distortion effects, and modelled using both one-dimesional (1D) and two-dimensional (2D) inversion codes. Finally, the results are interpreted in terms of the known geological features of the region.

Geological setting

The following simplified discussion of the geology of the region is based on the accounts of Bally et al. (1966), Harrison (1972), Monger and Price (1979), Price (1981), Coney et al. (1980), Cook et al. (1988), Coney (1989), and Yoos et al. (1991). The Foreland Belt formed during much of the mid to late Palaeozoic and early Mesozoic eras from the northeastward thrusting and folding of crystalline basement rocks, together with carbonate and clastic sediments, deposited in a long-lived miogeocline on the western boundary of cratonic North America. Bally et al. (1966) divided the Foreland Belt of southeastern British Columbia and adjacent Montana into four regions (Fig. 2*a*), which, from east to west, are the Foothills belt (FB), the Front Ranges (FR), the Rocky Mountain trench (RMT), and the Purcell Anticlinorium (PA) of the Purcell Belt.

The Purcell Anticlinorium is a structural high consisting of Belt Supergroup rocks deformed by a series of north-northwest-trending folds and faults. It is characterized by high heat flow, extensive reflectivity, and high electrical conductivity (Cook and Van der Velden 1995). According to Cook and Jones (1995), whereas the high reflectivity is mainly caused by the impedance contrast between the interlayed mafic sills and the low-grade metasedimentary rocks of the anticlinorium, the high electrical conductivity is most probably due to the presence of sulphide-rich layers within the metasedimentary rocks, as has been observed in the Sullivan mines near Kimberley (Hamilton et al. 1981).

Most of the MT profile lines cross the Lower, Middle, and Upper Belt–Purcell strata, where, besides numerous faults, other notable geological features lie. Koocanusa line 1 (D) crosses the Libby thrust belt (LTB) and the Rocky Mountain trench (Fig. 2*b*), a topographic low bounded on the east by normal faults. Koocanusa line 5 (E) passes in the area of the Bristow Creek (BRC) and Kootenay River (KR) fault systems and the Pinkham thrust (PT). Koocanusa line 9 (F) passes through the area of the Fairvie Anticline (FA). A deep petroleum exploration well, the ARCO 1 Paul Gibbs (location shown in Fig. 2*b*), was drilled in 1983 and 1984 to a depth of 5417 m (Boberg 1985). Interpretation of seismic data and results from this well led Yoos et al. (1991) to suggest that 15–22 km of Precambrian Belt Supergroup sedimentary rocks are present in several thrust plates in this region of the Purcell Anticlinorium.

The sedimentary strata in the Purcell Belt basin (also known as Belt–Purcell Supergroup) developed in a 600 Ma time span (between about 1450 and 850 Ma) on, and adjacent to, the flood plain of a large subsiding delta along the western margin of the North American craton (Price 1964; Harrison 1972). The Belt–Purcell Supergroup rocks are subdivided into four groups (Fig. 3), which, from base to top, are (*i*) Lower Belt, the Prichard Formation (also known as the Aldridge Formation); (*ii*) the Ravalli Group; (*iii*) the Helena and Wallace formations (Middle Belt carbonates); and (*iv*) the Missoula Group (Harrison et al. 1972). All of these units thin eastward. Mainly, these units consist of argillite, siltite and siltstone, dolomite and limestone, quartzite, and greywacke-like rock assemblages.

Fig. 1. The study area in which magnetotelluric soundings have been made, in relation to the five morphogeographic belts of the North American Cordillera.

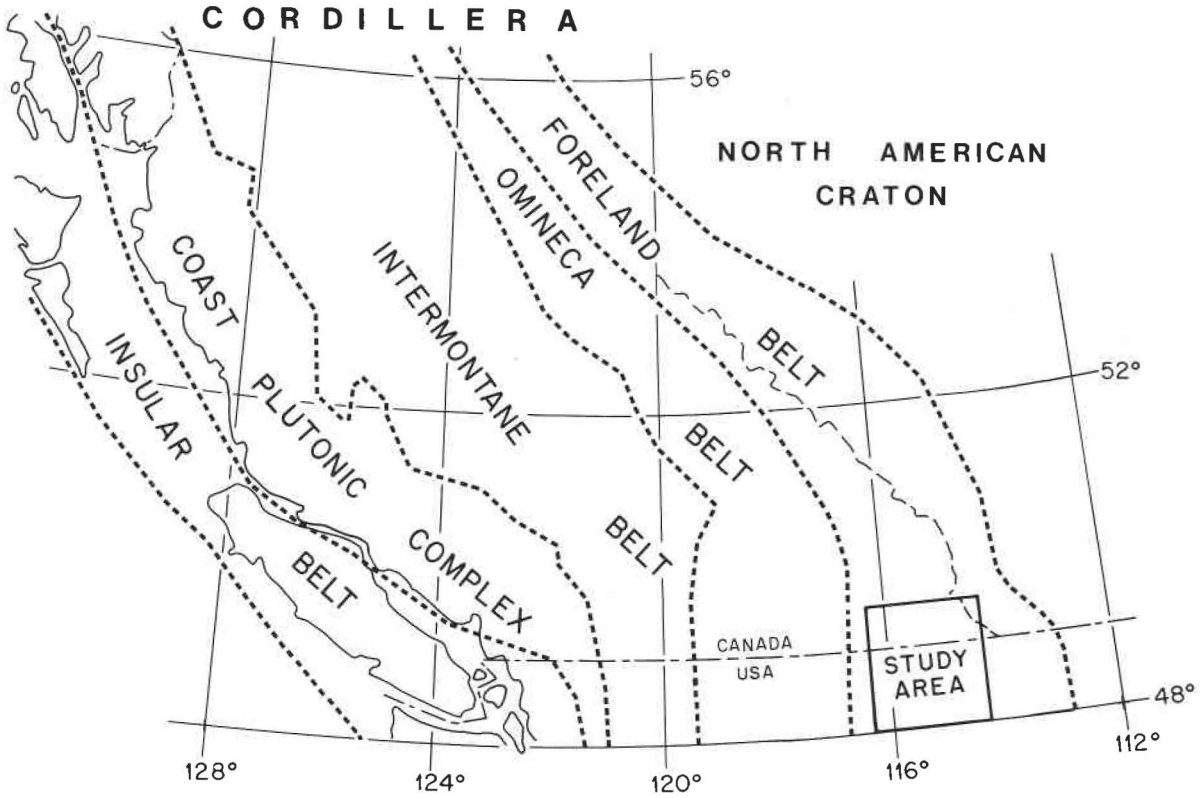

The belt is rich in minerals throughout its thickness. Large amounts of copper (100 or more ppm) are found in all the formations throughout the Purcell basin (Harrison 1972, his Fig. 12). The principal copper minerals are chalcopyrite, chalcocite, and bornite, and are commonly accompanied by covellite and various secondary hydrous copper minerals. Locally, however, the copper is more concentrated in thin beds or argillites or limestone. This extensive lateral and vertical distribution indicates that copper was originally introduced into the rocks as an element either syngenetically or diagenetically.

In northwestern Montana the Prichard Formation contains several graphitic units and zones of high pyrite–pyrrhotite, and specimens from some localities contain as much as 10% disseminated sulphides (Wynn et al. 1977).

In the rocks of the Ravalli Group, economic concentrations of copper exist and depths on both the eastern and western sides. Ore-grade copper (10 000 – 20 000 ppm) is found in the western Montana "copper sulphide belt," extending to about 65 km east from the Idaho–Montana border, from the vicinity of the 48th parallel northwards close to the Canadian border (see Fig. 14). It exists in siltites and especially in the coarse blocky quartzite layers, particularly the uppermost quartzite, of the Revett Formation (the upper part of the Ravalli Group, Fig. 3). In the area of investigation, the Revett Formation is less than a kilometre thick, and its depth increases eastward from about 4 to 9 km.

Middle Belt carbonate rocks in the Helena and Wallace formations generally contain abundant deposits of hematite and chalcopyrite crystals and blebs as anomalous copper concentrations. Secondary copper minerals, and locally some of the primary copper sulphides, can also be found in small fractures in many occurrences.

In the upper part of the supergroup rocks, i.e., in the Missoula Group, copper appears to be more abundant in the eastern rather than in the western part of the basin. Specifically, the Snowslip and Shepard formations commonly contain several parts per million of copper. This has been attributed to the higher copper content of the eastern source area.

Previous electromagnetic work

Wynn et al. (1977) interpreted shallow-penetrating audio-frequency magnetotelluric (AMT) data from a 45 km long profile located close to our Koocanusa line 9. Their AMT data were not collected at sufficiently low frequencies to penetrate the crystalline basement, but they did resolve several intermediate structural features and a deep layer of unusually high conductivity. For most of the British Columbian MT data used in the present investigation, Keller et al. (1990) examined the pseudoinversion ("Bostick") resistivity–depth curves. They noted that in this region, a highly resistive ($>1000\ \Omega \cdot m$) surface layer is underlain by a conductor to depths of a few kilometres. Beneath it, more resistive rocks were found that became progressively more conductive at depths greater than 10 km.

In a region about 500 km north of the present area of investigation, near the latitude of 53°N, MT studies of the Rocky Mountain trench were carried out by Hutton et al. (1987). For the upper crust they found resistivities of the order of $1-10\ \Omega \cdot m$ under the Rocky Mountain trench and even lower values under the adjacent Main Ranges (MR,

Fig. 2*a*). They interpreted this low-resistivity structure to be a thickening of the eastern edge of the Canadian Cordilleran Regional (CCR) conductor (Gough 1986), discovered in the early 1960's (see brief historical review in Marquis et al. 1995), and considered the probable cause of its high conductivity to be hot, saline water of mantle origin. More recently, the MT results of Jones et al. (1992), from an area just to the north of the present region, indicate that in the Foreland Belt the crustal conductivity increases from east to west.

Magnetotelluric data and analysis

Images of electrical conductivity variations derived from measurements of electric fields induced in the Earth by natural time-varying electromagnetic sources, caused predominantly by lightning activity at frequencies above 8 Hz and solar activity at frequencies below, furnish a view of the interior of the Earth complementary to that provided by seismic methods (e.g., Jones 1992). As part of geophysical studies of the Purcell Anticlinorium, MT soundings were carried out in the study area to determine the lateral and vertical spatial variation of this electrical parameter. Extensive high-quality seismic and MT data (almost 100 sites) in southeastern British Columbia, collected in the mid-1980's by commercial contractors for Duncan Exploration Co. (Denver, Colo.), were donated to the Lithoprobe project (Clowes et al. 1992) by Duncan. In addition, access to data from the 90 sites of a speculation MT survey of the anticlinorium in Montana, conducted by Phoenix Geophysics Ltd. (Toronto, Ont.) in 1984, was acquired by Lithoprobe and the Geological Survey of Canada.

These almost 200 sites lie on 15 east–west survey lines. Eleven of these survey lines are listed in Table 1 (from north to south) and consist of 168 MT sites; together these lines provide a reasonable grid suitable for a three-dimensional (3D) study of the electrical structure of the region (Fig. 2). They cross the Purcell Anticlinorium approximately perpendicular to its axis. Seven of these lines are referred to in the text using their designated letters.

Some results from the composite "Longfarrell line," where sites from the Farrell Creek and Teepee Creek are combined, are also discussed in the text. A well drilled by Duncan Exploration Co., known as the Moyie well (DEI-MOYIE D-8-C/82-G-5, 49°15′29.34″N, 115°50′27.46″W, depth ≈ 3500 m), lies near a site on this line, and the resistivity information from the well log has been used as control in the 2D modelling of the data from this line.

For the majority of the stations, MT data were acquired over almost six decades in frequency from 384 Hz to 1820 s, and were processed to obtain estimates of tensor impedances and the vertical magnetic field transfer functions. However, at most sites, the reliable data lie in the range 100 Hz to 100 s; the data scatter and error estimates outside of this range were deemed too large to warrant further analysis and subsequent interpretation. For some stations in the Duncan Exploration Co. dataset, only high-frequency data, in the range 384–1 Hz, were acquired. Data from about 20% of the sites exhibit 3D effects in the phases: in a geographic coordinate system phases for a certain frequency range lie in the second or fourth complex quadrant, whereas they should lie in the first and third for the off-diagonal elements of the MT impedance tensor (Z_{xy} and Z_{yx}), respectively. In most cases, these out-of-quadrant phases were observed in the low-frequency (long-period) part of the data, but in a few cases phases deviated into the wrong quadrant near 1 s period. These effects arise due to the deflection of electrical currents by the near-surface, inhomogeneous features, predominantly resistive anomalies but also conductive ones, in the vicinity of the sites (see Jones et al. 1988; Gupta and Jones 1990; Groom et al. 1993).

Table 1. List of survey lines from north to south.

Profile name	No. of MT sites	Designation in Fig. 2
Lumberton Road	20	A
Lamb Creek	8	
Farrell Creek	11	B
Teepee Creek	6	B
Sunrise Creek	5	
Sundown Creek	5	
Caven Creek	17	C
Ward Creek	6	
Koocanusa line 1	30	D
Koocanusa line 5	30	E
Koocanusa line 9	30	F

Notes: Sites from Farrell and Teepee creeks are combined to form Longfarrell line.

The regional geoelectric strike direction is determined by the extended version of the Groom–Bailey analysis (Groom and Bailey 1989) by McNeice (1994) and McNeice and Jones,[3] which determines the most consistent regional electric parameters over a range of frequencies and for multiple sites. The distortions of the regional data are caused by charge accumulations on electrical boundaries of surficial inhomogeneities. The distortion model assumed in Groom–Bailey analysis is of a galvanic 3D distorting sheet overlying a regional 2D Earth, and the parameters that are recoverable are the regional 2D impedances, the strike of the 2D body, and descriptors of the electric distortion (e.g., Jones and Groom 1993; Groom et al. 1993; Jones and Dumas 1993; Jones et al. 1993; Eisel and Bahr 1993). The unconstrained Groom–Bailey strike directions for each site, with inherent $\pi/2$ ambiguity, determined over a decade of frequency are displayed in Fig. 4 for each site in five bands, namely, 100–10 Hz, 10–1 Hz, 1–10 s, 10–100 s, and 100–1000 s. The fit of the data to the assumed distortion model is indicated by the length of the arrow: large arrows show that the distortion model is an acceptable description of the data. Short arrows, indicative of large misfit between the data and the assumed distortion model, are either a consequence of overly optimistic (too small) error estimates or an indication that the data are influenced by large-scale 3D structures.

There is remarkable consistency in the strike directions, and the galvanic distortion model fits the data well at most of the sites throughout the region at frequencies above 1 Hz. This remains generally true also for periods longer than 1 s, except that some shorter arrows are noted in the middle of Lumberton Road profile, at the Rocky Mountain trench on

[3] G. McNeice and A.G. Jones. Multi-site, multi-frequency Groom–Bailey distortion analyses. In preparation.

Fig. 2. (*a*) Major tectonic and selected structural features of the Cordilleran Foreland thrust belt (based on Yoos et al. 1991). FB, Foothills belt; FR, Front Ranges; MR, Main Ranges; RMT, Rocky Mountain trench; PA, Purcell Anticlinorium; MOT, Moyie thrust; SMF, St. Mary fault; PUTR, Purcell trench; PRC, Priest River Complex. (*b*) Geological map of the part of the Foreland thrust and fold belt of the North American Cordillera between 48 and 50°N latitude (based on Price 1981; Yoos et al. 1991). Major geologic features and structures from east to west: LT, Lewis thrust; FF, Flathead fault; KB, Kishenehn basin; MT, MacDonald thrust; RMT, Rocky Mountain trench; PT, Pinkham thrust; FA, Fairvie Anticline; KR, Kootenay River; LTB, Libby thrust belt;

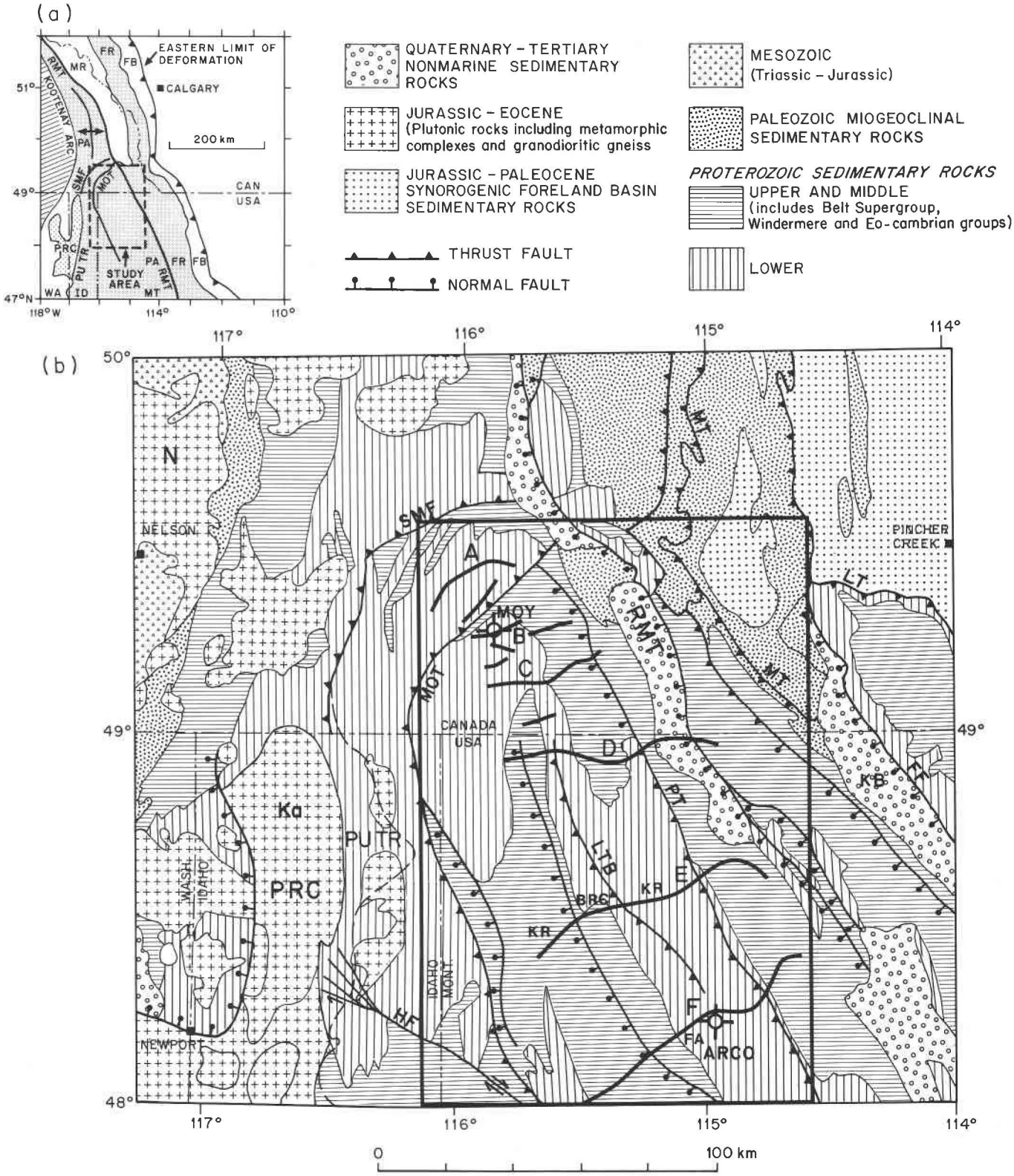

BRC, Bristow Creek; MOT, Moyie thrust; SMF, St. Mary fault; HF, Hope fault; PUTR, Purcell trench; Ka, Kaniksu batholith; N, Nelson batholith. ARCO, ARCO 1 Paul Gibbs Petroleum exploration well; MOY, DEI-MOYIE D-8-C/82-G-5 exploration well. Eleven survey lines, consisting of 168 MT data sites, cross the Precambrian Purcell Anticlinorium approximately perpendicular to the axis of the structure. The following six lines have been renamed lines A–F: A, Lumberton Road; B, Longfarrell; C, Caven Creek; D, Koocanusa line 1; E, Koocanusa line 5; F, Koocanusa line 9. These lines provide a reasonable grid suitable for 3D study of the electrical structure of the region.

Fig. 3. Representation of the Foreland Belt Supergroup with special emphasis on the Belt–Purcell Supergroup.

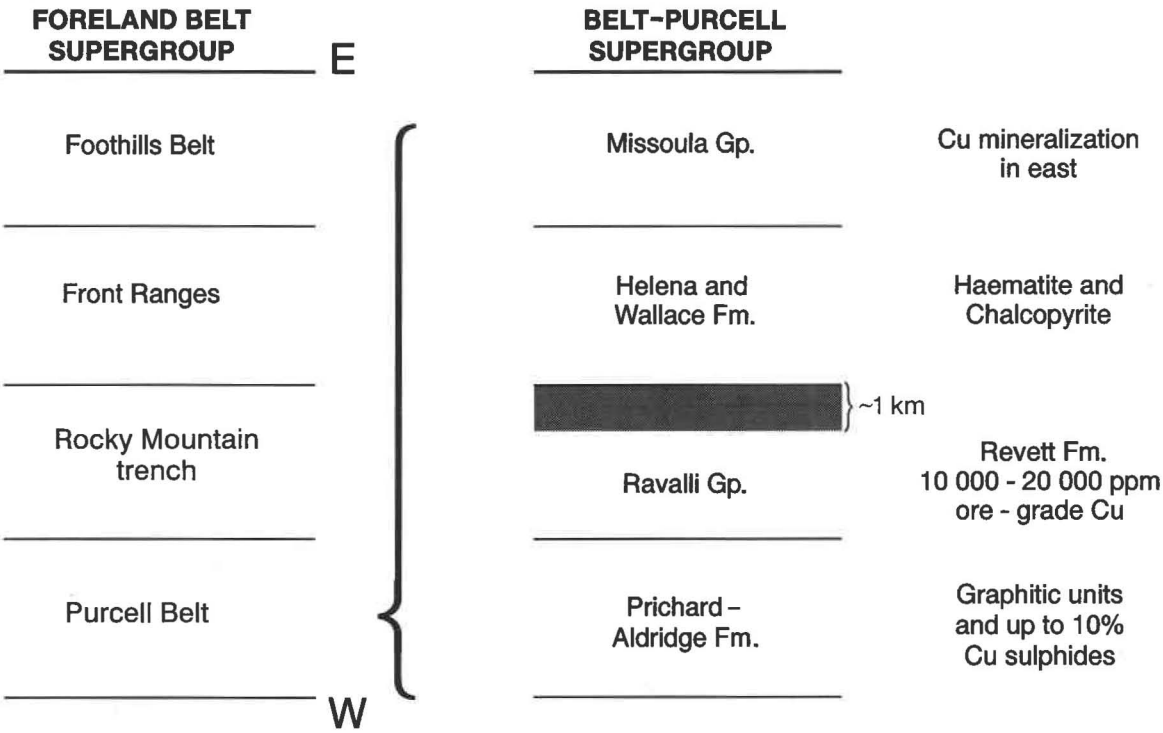

Koocanusa line 1, at the region of the Kootenay River and nearby faults on Koocanusa line 5, and in the area of the Fairvie Anticline of Koocanusa line 9. This large misfit is likely caused by the presence of some large-scale 3D structures within the sensing range of those sites (either laterally or deep within the crust). At these longer periods some counterclockwise rotation of the arrows is also evident, especially at the sites along the Lumberton Road profile. This distortion analysis suggests that the geoelectrical strike direction is, in general, consistent with the predominant surficial geological trend of the region. One significant departure is apparent in the northernmost part of the region, where the deeper electrical structures evidently strike more to the west.

Figure 5 displays the strike directions determined from the data from each site for each profile in the range 100 Hz to 100 s in circular histograms. For the end profiles, Lumberton Road, Longfarrell, and the Koocanusa line 9, the strike directions are well defined and lie near $-30°$, but for the intermediate profiles the spread in strike directions is large. Such a spread in strike direction will occur over 1D or weakly 2D structures that have no preferred azimuth (to within the error tolerances of the data). It will be shown below that the middle crust beneath these lines is very conducting, which results in limited penetration of the electromagnetic (EM) fields. Thus, the fields sense only the upper and middle crust, which can be modelled validly in 1D. Taking into consideration the results shown in Figs. 4 and 5, together with the regional geological trend shown in Fig. 2, we conclude that where the region exhibits a geoelectrical strike it is consistent with the local surface structural trends. Accordingly, the interpretation coordinate system chosen for these data is with a strike of $-30°$. For further analyses, the E-polarization (TE mode) and B-polarization (TM mode) results of the apparent resistivity (ρ_a) and phase (Φ) are descriptive of MT impedances data in the N30°W and N60°E directions, respectively. The Z_{xy} MT impedance element denotes TE-mode response, and is due to an electric field in a N30°W direction with a magnetic field in a N60°E direction; and vice versa for the Z_{yx} (TM-mode) element. Following the cautionary remarks in Jones and Groom (1993), the data from Longfarrell profile were not rotated into our adopted coordinate system, but were fitted to distortion models to obtain the regional 2D responses.

As a further consequence of local distortions, when in the correct regional 2D frame the data are also influenced by static shift, an amplitude-scaling effect of the apparent resistivity (ρ_a) curves. This effect displaces apparent resistivities up or down over a whole range of frequencies by a frequency-independent multiplicative constant, but leaves the phase curves unaffected (Jones 1988). At a site over a layered

Fig. 4. Strike directions calculated for five period bands: (*a*) 100−10 Hz; (*b*) 10−1 Hz; (*c*) 1−10 s; (*d*) 10−100 s; and (*e*) 100−1000 s. The length of an arrow is a measure of the fit of the data to a Groom−Bailey distortion model calculated for the 1D or 2D Earth under the influence of a 3D body that distorts the electric field only: long arrows indicate a good fit between the data and the model and the short arrows imply a poor fit between the two.

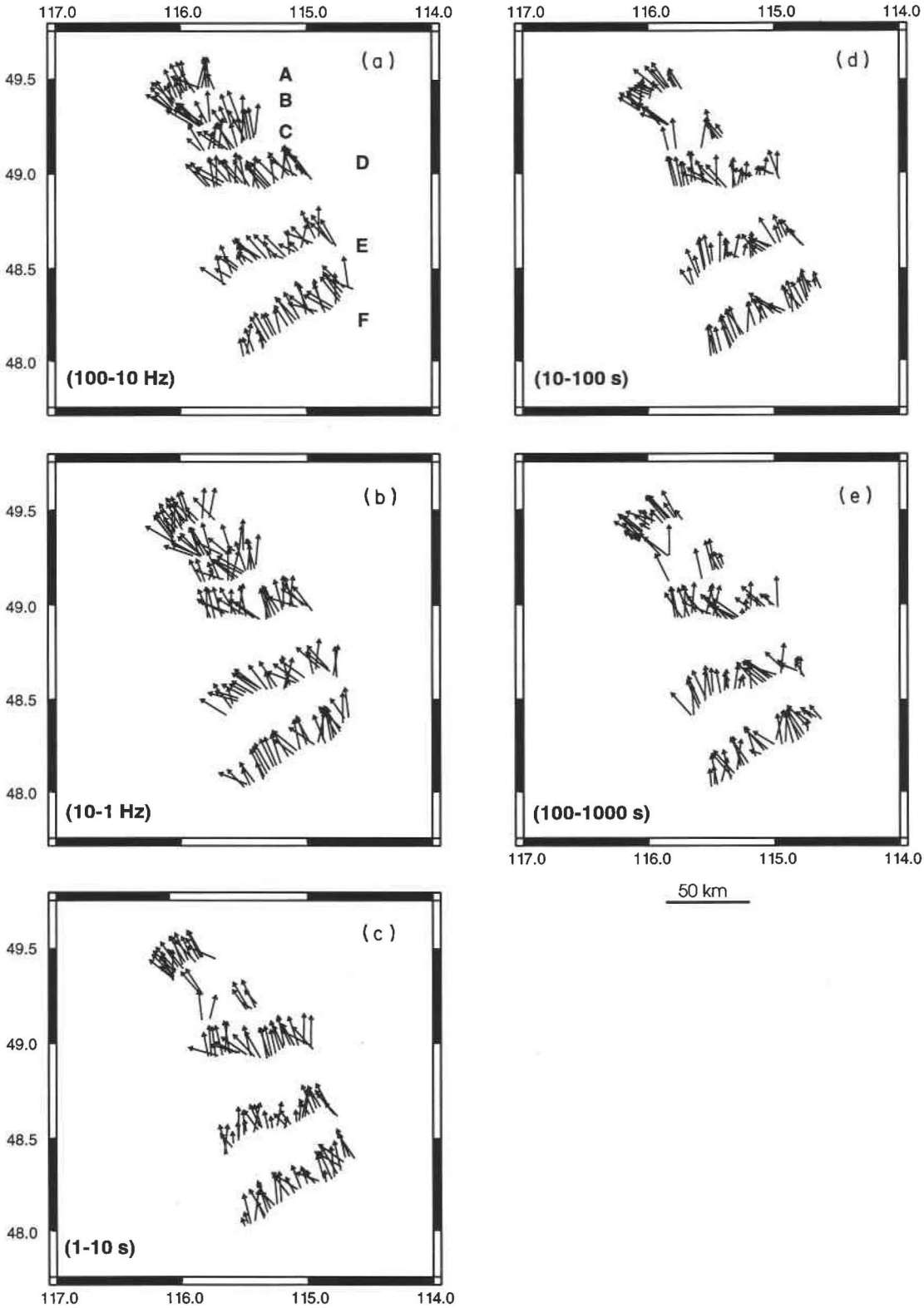

Earth, static shift becomes readily apparent when the phase curves are similar and the log apparent resistivity curves are parallel or nearly so, but are at different levels. Its effects are more prevalent at sites near resistive terrains than on the less resistive sedimentary areas (e.g., Gupta and Jones 1990). At a given site, static-shift effects must be removed to minimize large errors in both the resistivity and depth estimations (Berdichevsky and Dimitriev 1976). Methods to correct for the static shift have been discussed by Jones (1988), Sternberg et al. (1988), and Craven et al. (1990).

For approximate imaging of the subsurface, we use the rotationally invariant effective (square root of the determinant) impedance introduced by Berdichevsky and Dimitriev (1976). The apparent resistivity and phase calculated from the effective impedance have been successfully used in many MT investigations to study the conductivity structure beneath a site, even in the presence of strong 2D or 3D near-surface anomalies (e.g., Ranganayaki 1984; Sule and Hutton 1986; Ingham 1988; Gupta and Jones 1990; Majorowicz and Gough 1991). The effective phase is unaffected by the galvanic effect of charges on local near-surface inhomogeneities and is an unbiased estimate of the true effective phase of the regional impedances (Jones et al. 1991, 1992). Due to these qualities, the effective phase is considered to be a reasonable qualitative indicator of the gross regional structure and will be discussed further below.

Effective phase pseudosections and maps

The lateral variation in conductivity can be inferred qualitatively using pseudosections of the effective phase, the plots of the phase at the sites of a survey line against frequency with a logarithmic ordinate scale (Jones et al. 1990, 1991, 1992). The use of the logarithmic scale is appropriate due to the exponential decay of electromagnetic fields with depth. Phase-contoured pseudosections give an indication of conductive structures relatively unaffected by static shifts. In contrast, the resistivity pseudosections often exhibit vertical contours between sites due to the static-shift effects that must be removed to avoid modelling errors.

For a uniform half space of any resistivity, the phase lead of the electric field over the magnetic field is 45°. Phases greater than 45° indicate a layer at depth more conductive than the one above it, and conversely, phases less than 45° indicate a subsurface layer more resistive than the one above it. Phases of 0 and 90° indicate changes to zones of perfect resistivity and perfect conductivity, respectively, and so are physical limits for MT phases from 1D Earth and 2D Earth.

In Fig. 6, determinant-phase pseudosections for the six representative profiles, namely Lumberton Road, Longfarrell, Caven Creek, and Koocanusa lines 1, 5, and 9, illustrate the variation in regional conductivity. All of these profiles lie on the Purcell Anticlinorium, and the eastern portion of Koocanusa line 1 crosses the Rocky Mountain trench (Fig. 2). Clearly, much of the crust under the survey lines exhibits increasing electrical conductivity with depth.

Some noteworthy results that can be obtained from this figure are given as follows:

(1) The phases beneath the sites on Lumberton Road, which lie entirely over the Lower Belt strata, are larger both above and below a thin horizontal layer at a depth represented by 1 s. Below this layer, the phases and hence the conductivity increase with depth, and more so on the western side than on the eastern side of the profile.

(2) On the eastern side of the Longfarrell profile, very low phases near the surface indicate the presence of highly resistive structures. Below these structures, the phases increase with decreasing frequency (increasing penetration depth) everywhere except near the western edge of the profile, where somewhat lower phases extend to the longest periods.

(3) Compared with the pseudosection of Lumberton Road, phases along Caven Creek near 1 s are larger than those for

Fig. 5. Rose diagrams (circular histograms) giving the variation of the best-fit Groom–Bailey regional azimuth in 10° intervals.

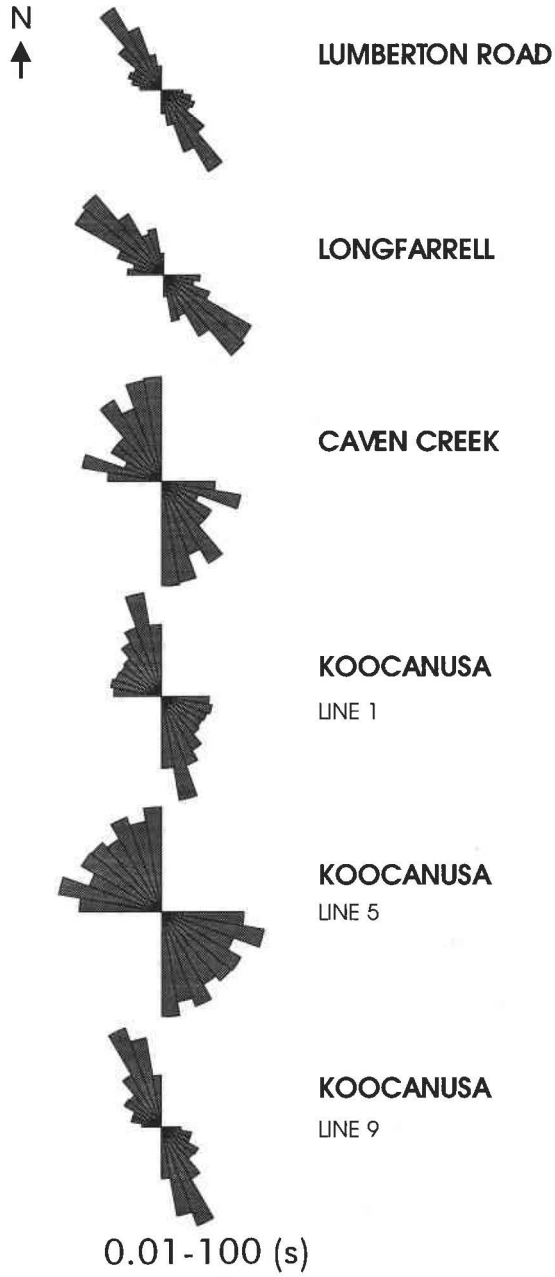

Fig. 6. Determinant-phase pseudosections for sites along the six chosen profiles. The scale infers that black is resistive strata and white conducting strata. L and UM refer to the Lower and the Upper and Middle Belt–Purcell strata, respectively.

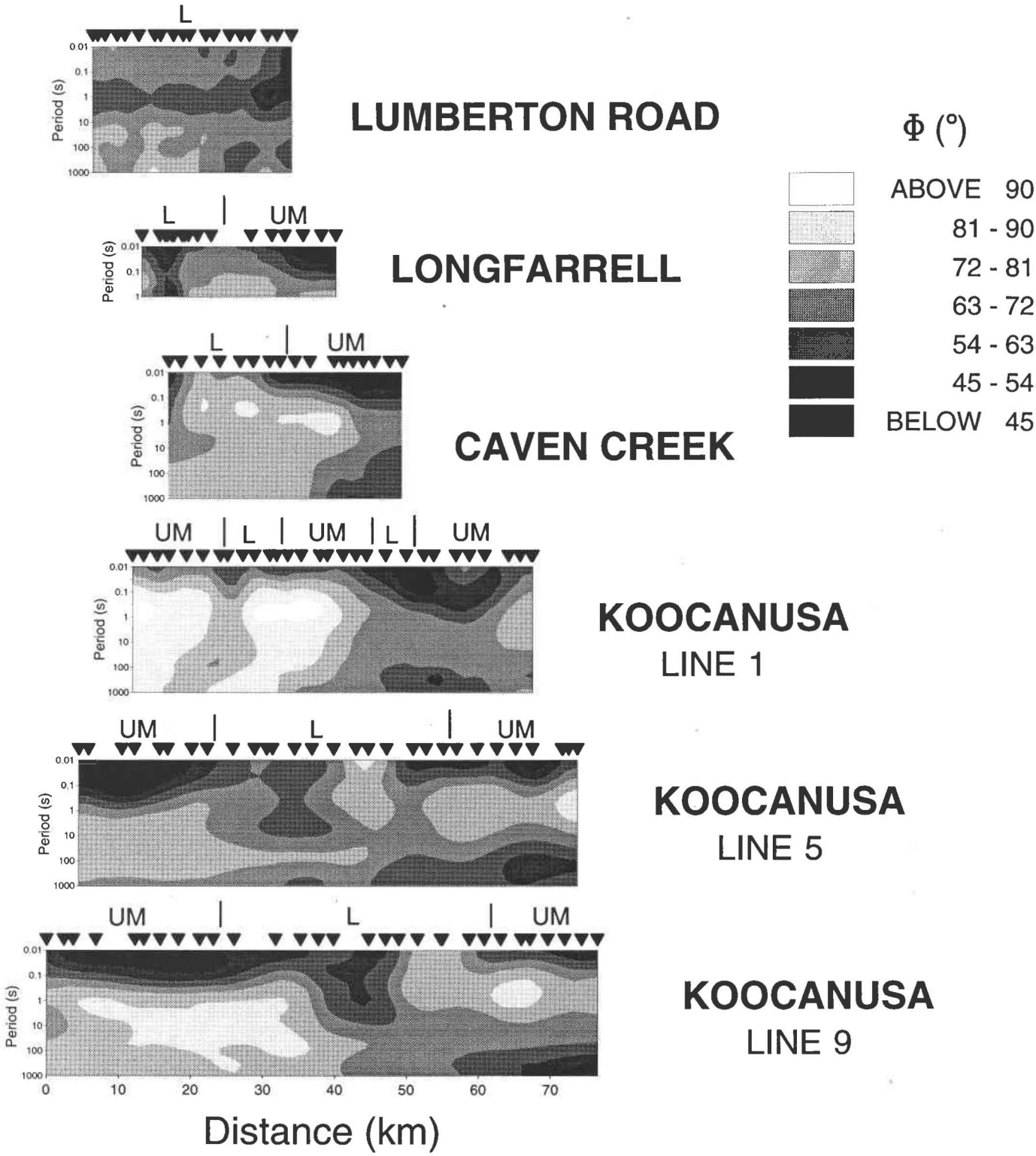

either the shorter or longer periods. This indicates a significant difference of the upper crustal structure beneath these two profiles.

(4) For Longfarrell, Caven Creek, Koocanusa line 5, and Koocanusa line 9, the identification of some resistive regions at short periods is well supported, as several adjacent sites show concomitant low phase values. Also at depth, in general, the sites of the profiles that lie on Upper and Middle Belt strata (UM in Fig. 6) exhibit considerably higher phases than those that lie on Lower Belt strata (L). This is clearly seen

Fig. 7. Contour maps of the $Z_{effective}$ phase at successively greater depths (longer periods). The phases greater than 45° are indicators of conducting regions and those less than 45° are indicators of resistive regions. Clearly, the western half of the area displayed is less conducting than the eastern half at shallow depths, but the converse is true for the deeper crust.

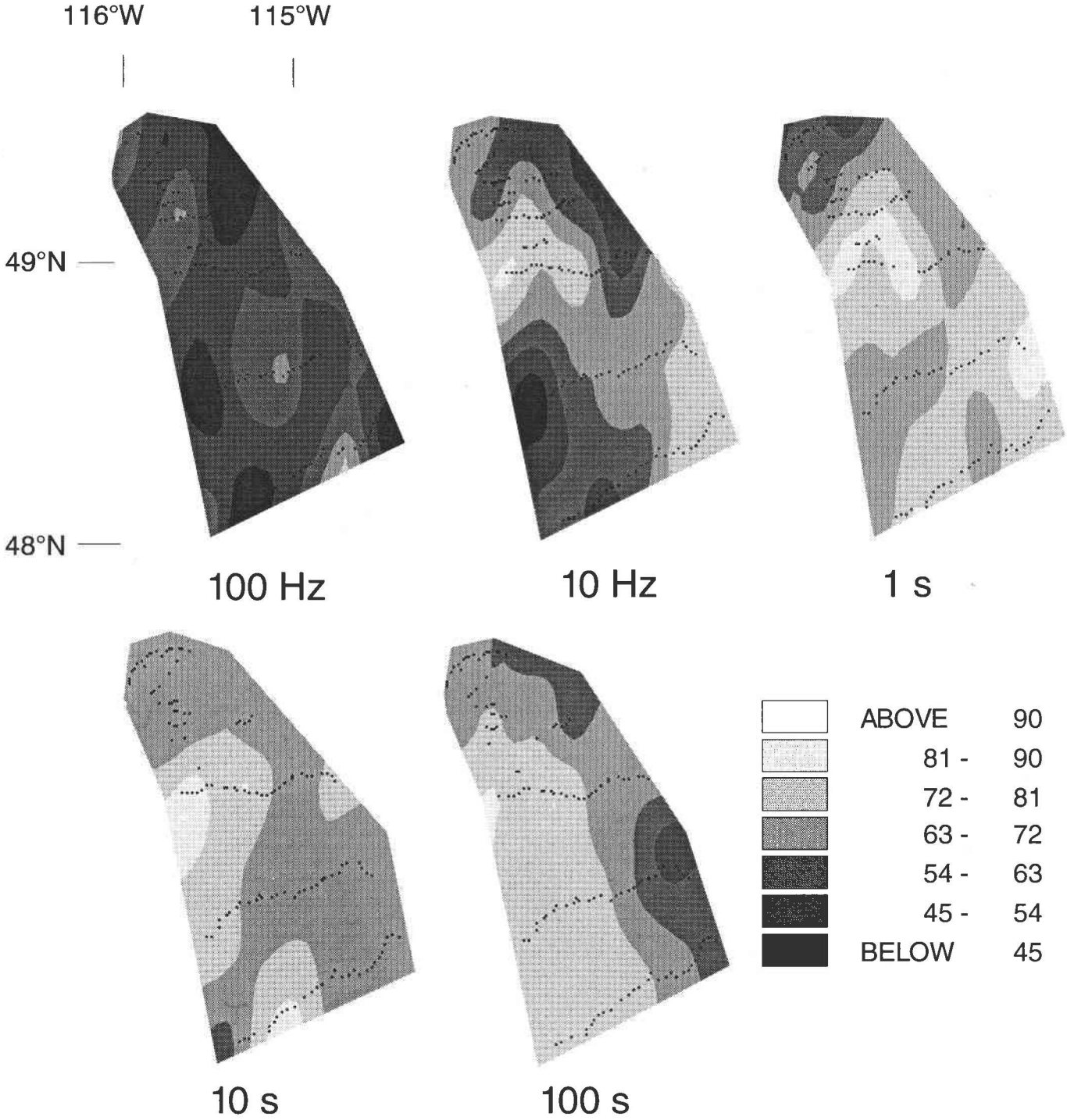

on Koocanusa line 1, which crosses the Upper and Middle Belt strata twice on the western side (Fig. 2*b*). This denotes that the sediments in the Upper and Middle Belt strata are generally more conducting than those in the Lower Belt strata.

The phases at longer periods are found to be larger on the western side than on the eastern side throughout the region. Also, except for the northernmost line, everywhere the phases for the midrange periods (close to 1 s) are larger than those for the short or long periods.

All the pseudosections of Fig. 6 display similar features, which prompts us to examine the phase variations at specific periods for the entire region. Maps of effective phases are shown in Fig. 7 for periods that approximately represent fea-

Fig. 8. Real induction arrows at 36 Hz, 18 Hz, and 1.33 s, from 11 western sites of Koocanusa line 1 beneath which two conducting conduits C1 and C2 are observed near the eastern and western edges of Libby thrust belt (LTB, Figs. 11 and 12).

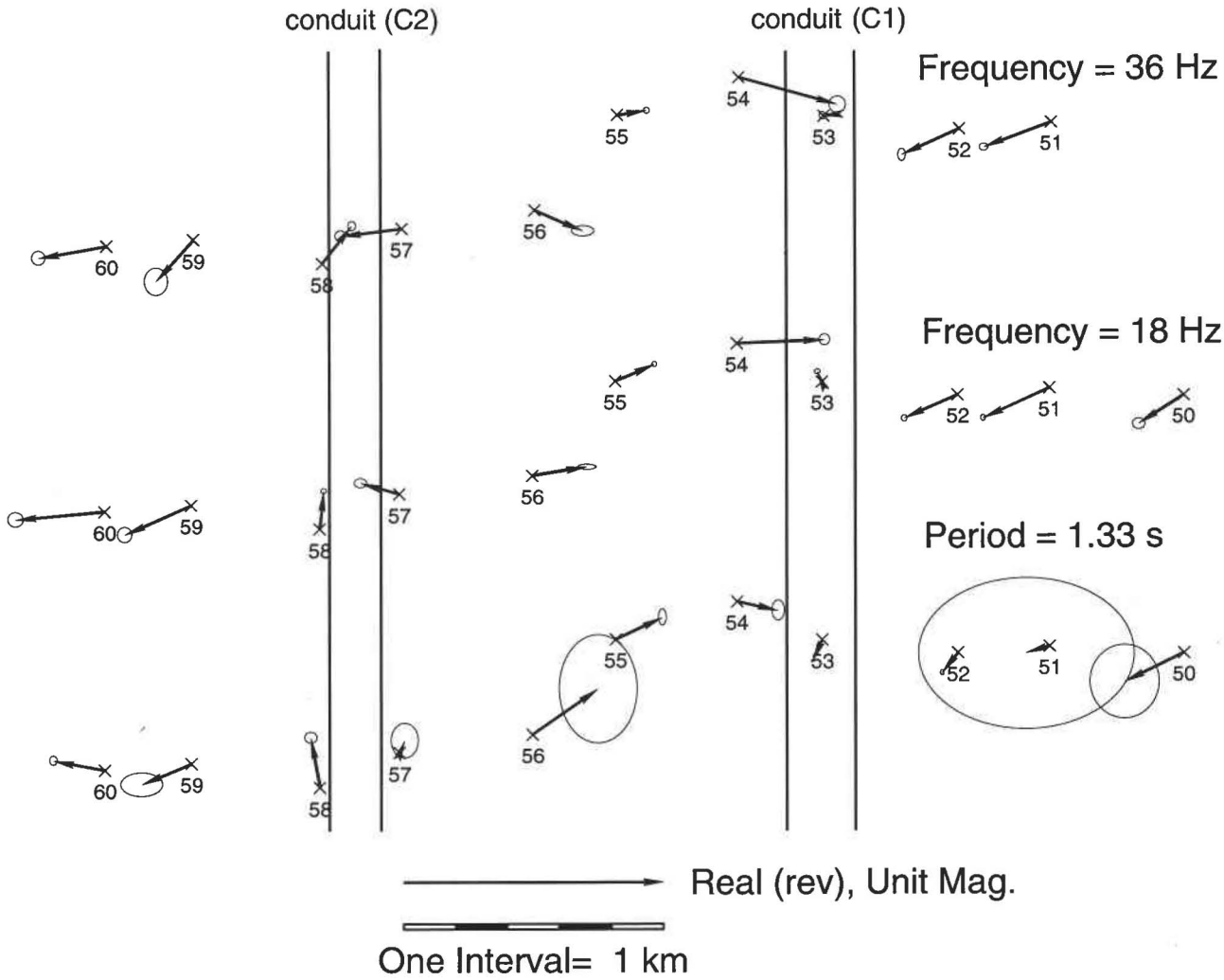

tures from the uppermost (1–2 km) to middle (15–20 km) crustal depths. At the highest frequencies (100 Hz), two conducting areas, one in the northwest and one in the southeast, and two resistive areas, one in the northeast and the other in the southwest, are apparent. With decreasing frequency, equivalent to increasing depth, the resistive areas decrease in lateral extent, and the conductive areas increase and become more conducting (higher phases). At depths corresponding to 1 s periods, the resistive areas become conducting, and the phases suggest that the one in the southwest near Koocanusa line 9 becomes about as equally conducting as the one in the northwest mentioned above. At depths corresponding to penetration of 10 s electromagnetic fields, the conductivity in the southeast decreases, but the western side becomes very conducting. At this depth, with the exception of a small area in the north, the western side of the region is more conducting than the eastern side. At 100 s period this contrast is enhanced and western side phases approach and exceed 80°, particularly in a wide northwest–southeast-trending strip at latitudes lower than that of Caven Creek.

This whole conducting region will henceforth be called the Purcell Anticlinorium conductor.

Induction arrows

The ratio of the vertical component to the horizontal magnetic field components can be expressed as an arrow, which usually points towards currents in conductivity concentrations (Parkinson 1959, 1962; Schmucker 1970; Jones 1986). Induction arrows, with error ellipses, were plotted for the data from the various profiles to identify conductive zones. For the Longfarrell profile, nearby power lines influenced the induction arrows at frequencies above 18 Hz. For lower frequencies the induction vectors behave in a manner expected of induction in subsurface structures. Figure 8 illustrates the induction arrows at certain frequencies from Koocanusa line 1 in the region of Libby thrust belt. On the western side of the profile, oppositely directed arrows suggest two narrow conducting bodies, conduits C1 and C2, lying close to the surface. Both of these bodies are also seen in the 2D inversion model of this profile discussed below (see Fig. 12), where they are noted to appear to rise upwards from a conductor below. The current concentration in these subvertical conductors is responsible for the oppositely directed induction arrows observed in Fig. 8. Conduit C1

appears to be more conducting than C2. In resistive terrains, similar conduits have been identified in previous surveys. A conduit observed by Mozley et al. (1986) was considered to be a channel electrically connecting a deep, highly conducting body to a surface conductor.

Resistivity pseudosections and static-shift corrections

To determine the actual variation of resistivity with depth, the regional undisturbed levels of apparent resistivity curves are needed. These regional levels of the MT apparent resistivity curves are affected by the conductivity variations near the surface (e.g., Jones et al. 1992), leading to static shifts of the observed apparent resistivity curves. An examination of the pseudosections (not shown) of apparent resistivity, obtained from the strike-parallel apparent resistivity (E polarization or TE mode) curves, showed that the contours are reasonably smooth and that they imply approximately the same crustal structures as suggested by the phase pseudosections of Fig. 6. This indicates that the static-shift effects on the TE-mode data are relatively small. However, to reduce the effects of static shifts, correction factors were calculated for the individual profiles, under the assumption that the Earth below a certain depth is 1D, which requires the TE-mode ρ_a data at some appropriate long period to follow a simple regional trend (e.g., Jones et al. 1992). This assumption was based on the discussion of Fig. 5, and also on the observation of a similarity of the TE- and TM-mode phases for several sites of a profile in a certain period band indicating that the corresponding Earth structure is 1D, i.e., horizontally layered. The calculation of the appropriate static-shift correction factors for the apparent resistivity data from each site along the different profiles was made as follows. The E-polarization resistivity data at 100 s from all of the sites on a profile were plotted together with their error bars (for the Longfarrell and Caven Creek profiles, due to lack of data above 1 s period for several sites, resistivities were considered at a period of 0.1 s). The outliers from a visualized general trend were identified and removed, and a quadratic curve was fit to the remaining points. The differences of the individual data points from the general trend of this quadratic curve provided the static-shift corrections to be applied at the individual sites, using the method suggested by Jones (1988) and adopted by Jones and Dumas (1993). Once the E-polarization data were made consistent with regional induction, the B-polarization data were corrected by shifting the curve such that the apparent resistivity data had the same short-period asymptote as the E-polarization curve.

As a check of this method of static-shift correction, we can compare the equivalent apparent resistivity curve derived from the electrical log of the Moyie well data with the static-shift-corrected resistivities obtained from the MT data of the nearest site (Fig. 9). The B-polarization curve (YX in Fig. 9) has a spectral shape that mimics the derived well-log response, and is offset from it by less than one-quarter decade. The E-polarization curve (XY) is much different in shape from the well-log synthetic curve: this is due to the 2D nature of the subsurface in the vicinity of the well. The split in the two curves is modelled in 2D (see fit in Fig. 13, site lon014), and the feature that causes this split is shown

Fig. 9. Resistivity values calculated from the well-log data and the static-shift corrected resistivity data from the nearest site lon014 on Longfarrell line.

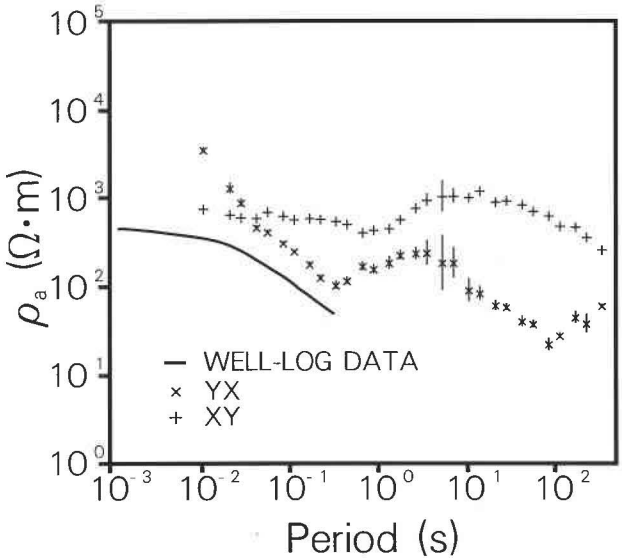

(see Fig. 12) as an "upwelling" of conducting material (this feature is modelled in more detail in Cook and Jones 1995).

The static-shift-corrected E-polarization apparent resistivity data are plotted in pseudosection form in Fig. 10. In general, the uppermost parts of the crust are resistive over the whole area, which corroborates the earlier observation of Wynn et al. (1977), who found a resistive upper crust near the eastern part of Koocanusa line 9, 0.5–7 km thick. Near to the middle of this line, the low-resistivity regions close to the surface are in the area of Fairvie Anticline (FA), where two known faults exist. Similarly, in the middle of Koocanusa line 5, the low-resistivity areas close to the surface lie in the vicinity of the fault systems of Bristow Creek (BRC) and between the Kootenay River (KR) and Pinkham thrust (PT). It is also worth noting that the resistivity pseudosection of Koocanusa line 1 clearly identifies the Rocky Mountain trench as a strong conductor with resistivity from less than 100 Ω · m near the surface to values near 1 Ω · m at greater depths. Similar low resistivities were reported previously for the Rocky Mountain trench farther north by Hutton et al. (1987). This observation also concurs with the study by Gupta and Jones (1990) of the odd geomagnetic transfer function data from Flathead basin. Gupta and Jones (1990) concluded that these geomagnetic depth sounding data indicated the existence of a low-resistivity zone in the middle to lower crust, about 50 km west of the Flathead basin, corresponding to the location of the Rocky Mountain trench.

One-dimensional modelling

To obtain better approximate images of the subsurface, and also as a preliminary step towards 2D inversion, after correcting the data for static shifts, the E-polarization apparent resistivity and phase curves were transformed from the period domain to the depth domain using the 1D Occam least structure code of Constable et al. (1987). The appropriate minimum misfit goal at each site was chosen using Parker's

Fig. 10. E-polarization apparent resistivity pseudosections obtained after static-shift corrections were made to the data by removal of quadratic-curve trend at a chosen long period of a profile. BRC, Bristow Creek; FA, Fairvie Anticline; KR, Kootenay River; LTB, Libby thrust belt; PT, Pinkham thrust; RMT, Rocky Mountain trench.

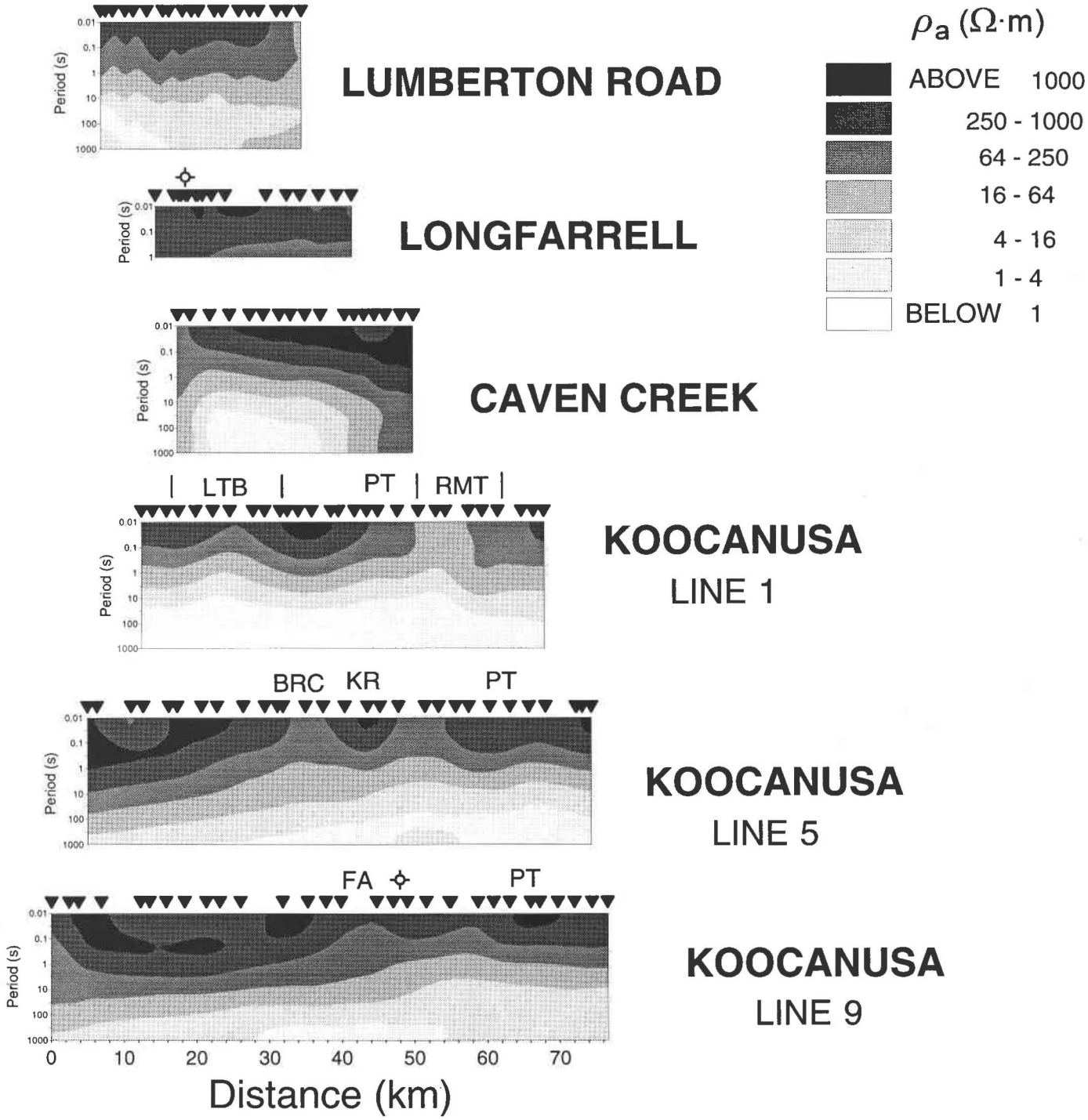

(1980) D^+ test, which gives the absolute minimum misfit possible for the data. Models were found which had χ^2 misfits that were 10% greater than the minimum possible, indicating excellent fit to the data. The 1D models are illustrated in Fig. 11 in a continuous section for each profile, i.e., the 1D models have been "stitched" together in pseudo-2D model format. It must be noted that these depth sections may not be true representations of 2D structure, as they are 1D approximations. In the following section we will explore the fidelity of these 1D images by comparing them with ones obtained using full 2D inversion techniques.

The resistivity variations noted in Fig. 10 are well reflected in Fig. 11. The western part of the region is, in general, more conducting than the eastern part. The part of Koocanusa line 1 section marked "no penetration" is so highly conducting that EM fields of period near 100 s and more cannot

Fig. 11. Depth sections obtained after static-shift-corrected apparent resistivity data (Fig. 10), and the phase data are transformed from the period domain to the depth domain using the 1D Occam inversion scheme of Constable et al. (1987). The white parts on various sections indicate regions of no penetration of EM fields. Abbreviations as in Fig. 10.

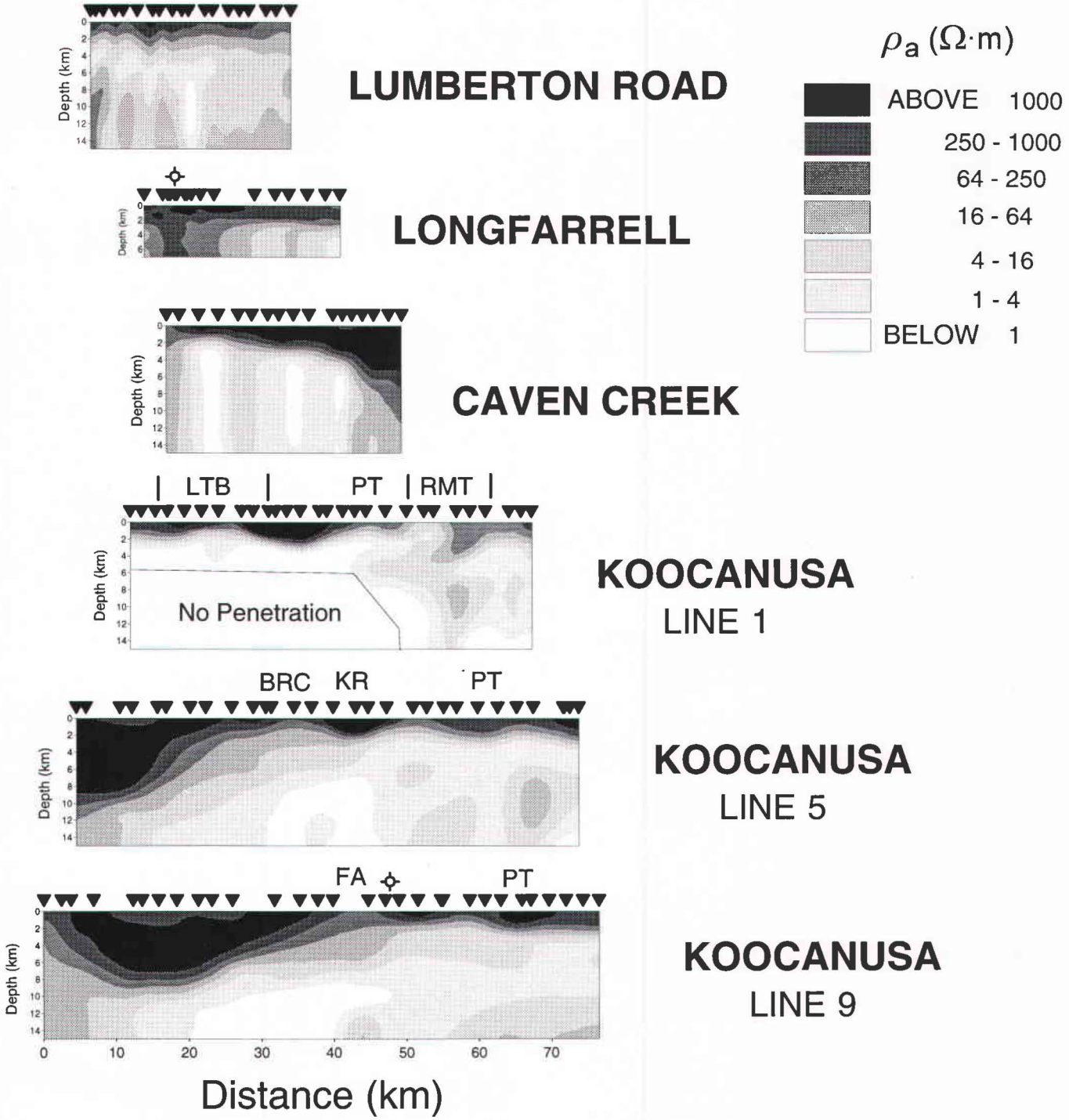

penetrate it. The conducting bodies approach the surface on Koocanusa line 9 in the area of Fairvie Anticline, on Koocanusa line 5 near the faults of the Kootenay River and the Bristow Creek, and on Koocanusa line 1 in the east beneath the sites of the Rocky Mountain trench and in the west beneath the sites in the area of Libby thrust belt. On the whole, the crust is very conducting over the region west of the Pinkham thrust (PT, Fig. 2*b*) below a few kilometres from the surface, and in several areas it is suggested that resistivities decreased to 1 Ω · m or less.

In the United States, the resistive terrains extend to depths of about 8–10 km on the western sides of Koocanusa lines 5 and 9, and to about 2 km on Koocanusa line 1, where beneath Libby thrust belt they flank a conducting zone that approaches the surface from below. In contrast, in Canada the resistive portion of the upper crust is thin under the Lumberton Road

Fig. 12. Two-dimensional models obtained by (*a*) RRI inversion of the structure beneath the Longfarrell line; and (*b*) Occam inversions for the structure beneath Koocanusa line 1, using both E- and B-polarization resistivities and phases from nine frequencies lying between 100 Hz and 100 s. Two conductive conduits C1 and C2 lie close to the borders of the Libby thrust belt (LTB).

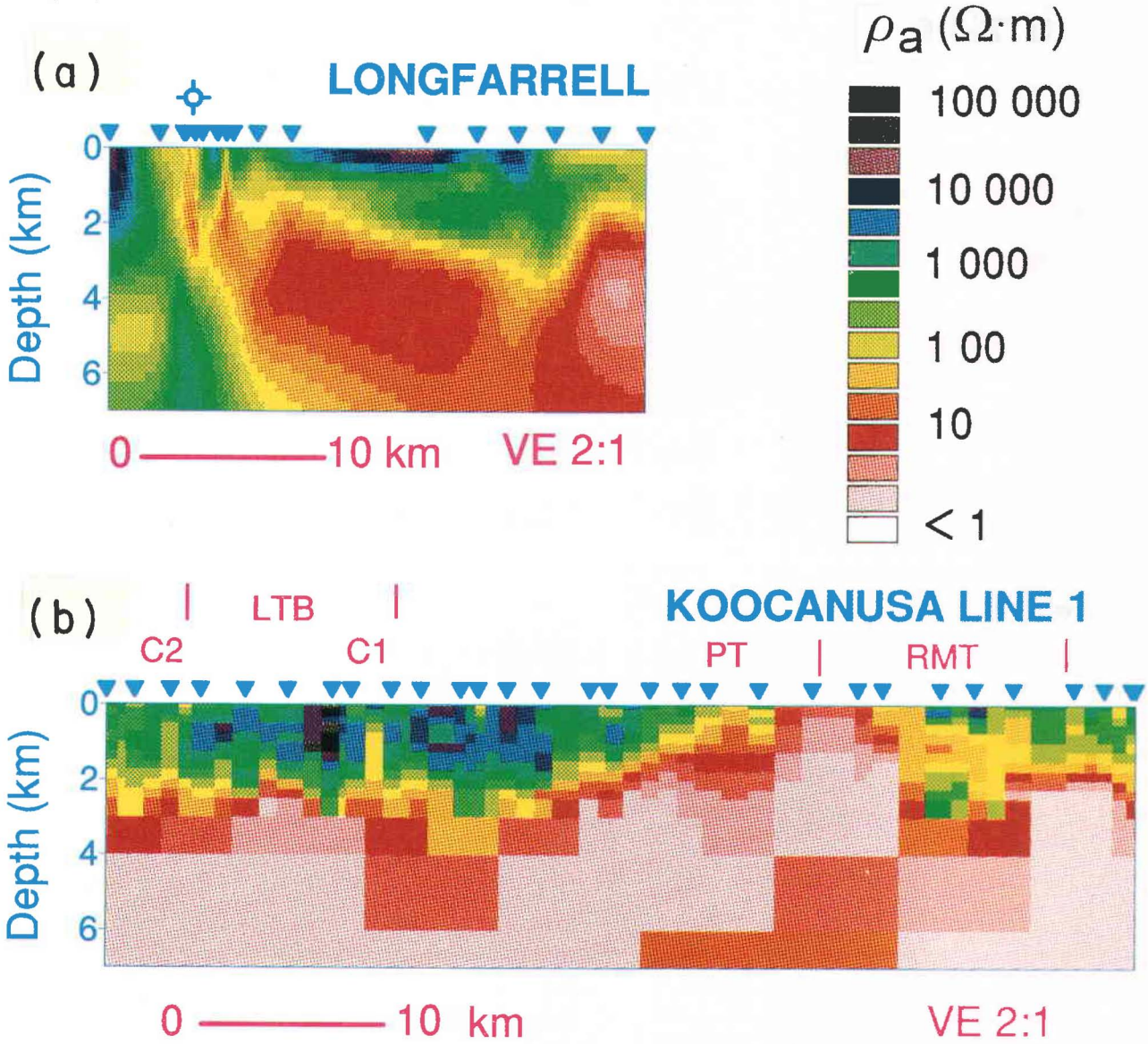

profile, is quite deep on the western side of the Longfarrell profile, and lies on the eastern sides of the Caven Creek profile where its maximum depth is about 6 km. The observed resistive regions may be due to Precambrian intrusive rocks that abound in the area to the west of the Pinkham thrust (PT). Their subsurface locations are discussed by Yoos et al. (1991, their Fig. 3), who used seismic reflection data, results from the data of the ARCO 1 Paul Gibbs well, and the down-dip projections of the surface crops, for interpretation.

Two-dimensional inversions

As noted above, the sections in Fig. 11 are only 1D approximations of the 2D Earth. To determine whether these 1D inversions represent well the 2D Earth, the data from two profiles, namely Longfarrell and Koocanusa line 1, were inverted using two methods for finding the smoothest model consistent with the data. These were the 2D Occam algorithm of deGroot-Hedlin and Constable (1990), modified by deGroot-Hedlin (1991), and the "rapid relaxation" inverse (RRI) of Smith and Booker (1991). The static-shift uncorrected, rotated data were two dimensionally inverted. Two different methods were adopted to account for the static shifts (see below); in one, the errors of the apparent resistivity data were increased, whereas in the other, the static shifts and smooth model were sought simultaneously.

As with all inversion problems, our data lead to models that are nonunique. However the two algorithms that we have used are based on the concept of finding "least-structure" models, i.e., best-fitting models are sought that also simultaneously minimize vertical and lateral gradient in conductivity. Accordingly, structures in the models can be more extreme than presented, in a conductivity-contrast sense, but not less so. Thus, these models represent the con-

servative end of the spectrum of acceptable models, and features in them are robust.

In the inversions of the data from the Koocanusa line 1 profile, greater weight was given to the MT phase responses, as they are unaffected by static shift. To achieve this, a very small error was permitted for the phase data, but the resistivity data were allowed to have a large error. This produced model ρ_a curves of the same shape as the observed ones, but not necessarily with the same level. Hence the model reflects regional trends in the resistivity variations without overfitting the local variations, caused by static-shifts.

The pseudosection of the Occam 1D inversions was used as a starting model for 2D inversion of the Koocanusa line 1 data, using the Occam 2D code. Data at nine frequencies equally spaced between 100 Hz and 100 s were taken, with an assumed error on the phase data of 1°, and on the ρ_a of 25%. Initially, the TE-mode data alone were inverted, and, after a few iterations, an rms of 5.99 was achieved, which did not reduce with later iterations. The resulting model was used as the start model for full 2D inversion of both the TE- and TM-mode data. After a few iterations, a stable value of rms = 8.41 was achieved, which implies that the model fits the data to within 8° on average. This final model is shown in Fig. 12*b*.

The data from the 17 sites on the Longfarrell line were inverted using rapid relaxation inversion. For most of the sites, all data in the range 100−1 Hz were used (14 frequencies). At four sites, data at six additional lower frequencies, to 10 s period, were available. Thus a total of 524 (= 2[(14 × 17) + (6 × 4)] data points were used. The assumed error floor was 2%, equal to 0.57° in phase, which is larger than the estimated error for more than half of the data. A half-space was used as a starting model. Using the approach for modelling static shifts expounded in Wu et al. (1993), smooth models were sought successively until the static shifts stabilized. For some sites, using a feature in a version of rapid relaxation inversion provided by T. Smith (personal communication, 1992), the same static shift was found for the TE-mode as for the TM-mode ρ_a, as their high-frequency ρ_a data overlapped, i.e., in Groom−Bailey parlance only the site gain, g, remained to be found. For other sites, the different shapes of the ρ_a curves for the two different modes of propagation suggested that there were inductive effects in the data. Holding the statics fixed at the stabilized values, a smooth model with low rms was sought. This model is illustrated in Fig. 12*a*. The rms misfit of this model to the data is 5.6, i.e., on average the model fits the phase data to within 3°. The observed data are compared with the model responses in Fig. 13. The calculated values from the models fit the observed resistivity and phase data well, and the misfits between the data and the model responses are generally well distributed among the sites of the profile.

Some features of the 2D models shown in Fig. 12 are as follows:

(1) Beneath the sites of Koocanusa line 1, a region of very high conductivity (10 Ω·m or less) is found below a depth of 2.5−3.0 km. Near the western boundary of the Rocky Mountain trench, this region gradually approaches the surface, where it is about 1−3 km wide. Near the eastern boundary of the Rocky Mountain trench, the conducting region also rises upwards, but only to a depth of about 1.5−2 km, and at its top it is again about 1−3 km wide. The conductor also rises upwards to a depth of about 2 km, a few kilometres west of the Pinkham thrust, below the Libby thrust belt. It is also noted that near the eastern and western boundaries of the Libby thrust belt conductive conduits C1 and C2, respectively, rise upwards towards the surface. As concluded earlier in the interpretation of the geomagnetic depth sounding transfer function data (Fig. 8), that conduit C1 is more conducting than conduit C2 is now corroborated by the MT data modelling. On the western side of the Rocky Mountain trench, west of the Pinkham thrust and encompassing the Libby thrust belt region, lies a very resistive terrain about 2 km thick. Most likely this is the terrain of Proterozoic sedimentary rocks that has been interpreted by Yoos et al. (1991) to contain an abundance of subsurface Precambrian intrusive rocks.

(2) Beneath the Longfarrell profile (Fig. 12*a*), a strong conductive region, at depths of around 2−3 km, approaches the surface in the region of the Moyie well. Comparison of the lithology from the rock chips and the electrical logs shows that this conductor is due to enriched sulphides lying within metasedimentary rocks (Cook and Jones 1995).

These two 2D models are close, in all major features, to the stitched 1D sections shown in Fig. 11. This suggests that for these data the 1D sections are reasonable approximations for all profiles.

Discussion

In the present investigation, the resistivities found in the Purcell Anticlinorium of the North American Cordillera range from over 5000 Ω·m, in some regions within a few kilometres from the surface, to less than 1 Ω·m, deeper in the crust. In the Purcell Belt, rocks are metamorphosed to greenschist facies, and the rock types found are greywacke, argillite, limestone, and siltite, most of which have high resistivities (Wynn et al. 1977). Their presence is quite likely the reason for high resistivities noted to depths of a few kilometres. The belt is also very rich in minerals to a considerable depth (see section Geological setting), and these mineralized zones have a strong influence on the MT data. Their presence appears to contribute in a major way to the observed highly conducting regions under the profiles.

The results of the present investigation of the electrical conductivity structure of the region may be summarized as follows:

(1) On average the strike of the conductive features is found to be N30°W (Figs. 4, 5), which is about the same as the surface geological trends for this region. However, there are some indications from Fig. 4*e* that at the latitude of the Lumberton Road profile, the geoelectrical strike is more westerly for longer periods (≥100 s) than for the short periods (see Figs. 4*a*, 4*b*).

(2) The sediments in Upper and Middle Belt−Purcell strata are more conducting than those in Lower Belt−Purcell strata. In general, beneath the surface to a depth of a few kilometres, the Purcell Belt is resistive, most probably due to the presence of a variety of metamorphosed rocks found throughout the region. The high resistivity implies that the near-surface rocks are dry. Below these rocks the Purcell

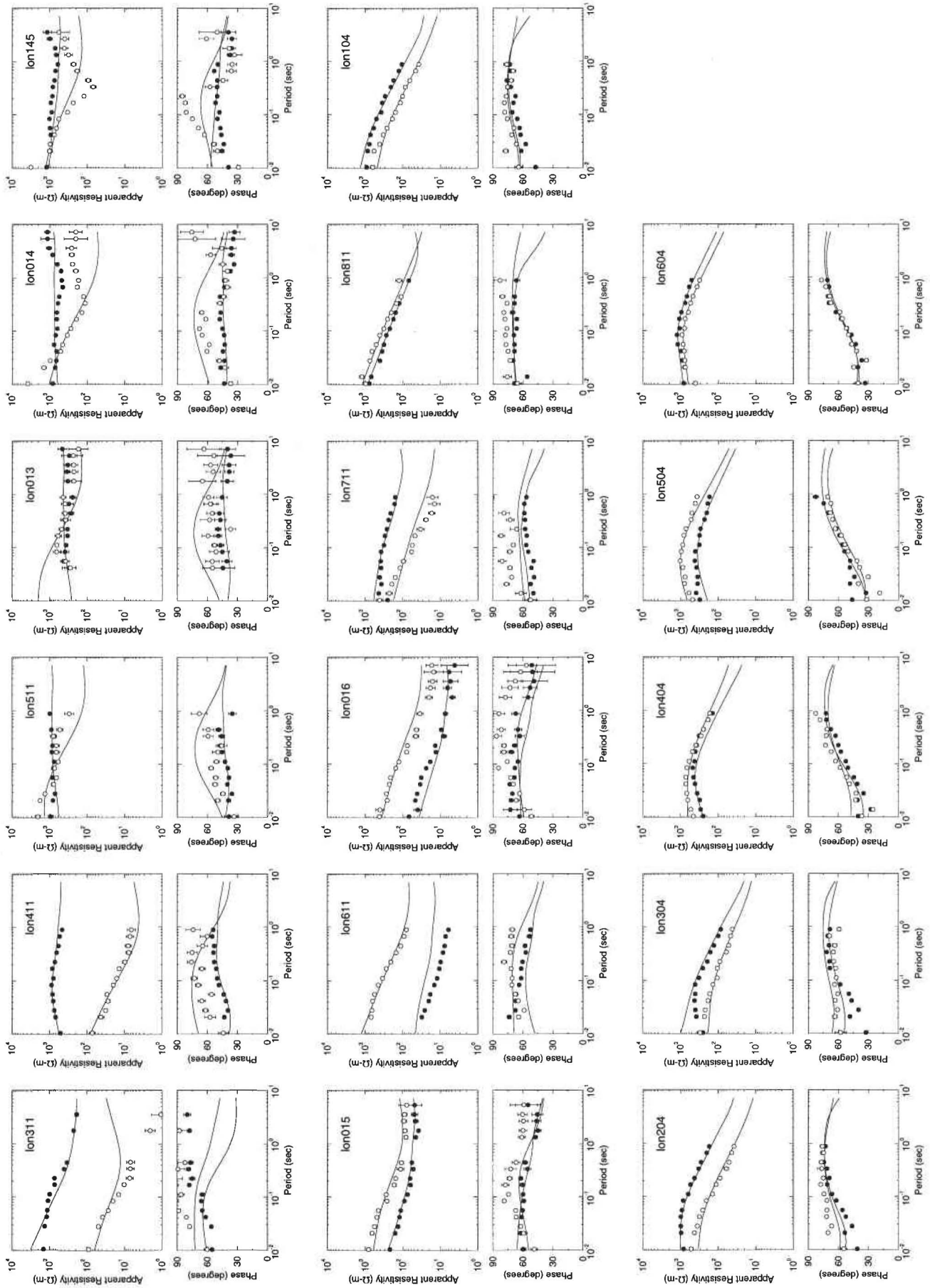

Fig. 13. A comparison of the E-polarization (●) and B-polarization (○) data with the model responses (solid lines) from the model given in Fig. 12*a* for Longfarrell profile. The westernmost site of the profile is lon311, and the easternmost lon604.

Belt is found to be highly conducting everywhere (see Figs. 10, 11), probably due to the presence of copper sulphide and other minerals (see Cook and Van der Velden 1994).
(3) The western part of the region appears to be relatively more conducting than the eastern part below a few kilometres from the surface (Figs. 7, 11). The most conducting region is present beneath Koocanusa line 1, where resistivities dropped to 1 $\Omega \cdot$m or less. The extent of the conducting regions, as well as their conductivities, decreases more rapidly northwards than southwards from this line. However, large conductivities extend to the Lumberton Road profile, indicating the possible continuation of the mineralization to these higher latitudes, although in significantly reduced quantities and in isolated areas only.
(4) The depth of the pervasive conducting layer changes considerably over the region. The conducting layer is closest to the surface (depth of $\sim$2 km) beneath Koocanusa line 1 and increases in depth both northwards and southwards (Fig. 11).
(5) The major features of the 2D inversion models of Fig. 12 are also in Fig. 11, which shows highly conducting regions ($\leq$1 $\Omega \cdot$m), below a few kilometres, under the various profiles. Also the 2D model for the Longfarrell profile indicates a subsurface conducting region in the vicinity of the Moyie well location. According to Cook and Van der Velden (1995) and Cook and Jones (1995), the measurements of the electrical resistivity of the rocks penetrated by the Moyie drill hole show that some of the sedimentary rocks lying between the resistive sills are extremely conductive, and in many cases resistivities less than 0.1 $\Omega \cdot$m are noted. These thin sedimentary layers are found to a considerable depth and their high conductivity is most probably due to the embedded metallic sulphide layers (Cook and Jones 1995). Sulphide-rich layers within the metasedimentary rocks to a depth of a few kilometres were also noted by Hamilton et al. (1981) for the Sullivan mines near Kimberley. The Purcell Anticlinorium is known to be very rich in minerals, and Fig. 14 shows that our area of investigation lies on the eastern side of the Montana copper sulphide mines (see Harrison 1972, his Fig. 14). From these facts, we conclude that the observed pervasive high conductivity in the region is due to some form of mineralization (possibly copper sulphide), rather than due to brines or graphite.
(6) This investigation confirms the presence of the Rocky Mountain trench conductor that was postulated earlier by Gough et al. (1982), Hutton et al. (1987), and Gupta and Jones (1990). As shown in Fig. 12, the trench is very conducting from close to the surface. The conductor (1–10 $\Omega \cdot$m) approaches the surface on the western edge of the trench, but its top is at a depth of about 2 km on the eastern edge. At its top, near both edges of the Rocky Mountain trench, the conductor is 2–3 km wide and it gradually widens downwards. From the present study, we conclude that mineralization in the trench is the cause for its high conductivity, as noted for the upper crust in other areas in this region (e.g., Gough and Majorowicz 1992). This interpretation is at variance with that from the study of the Rocky Mountain trench 500 km farther north where hot saline water of mantle origin was considered to be the primary cause of enhanced conductivity (Hutton et al. 1987).
(7) Near each of the boundaries of the Libby thrust belt a conduit containing conductive material ($\sim$100 $\Omega \cdot$m) has been found in the highly resistive medium lying west of the Rocky Mountain trench (Fig. 12). The presence of the conduits C1 and C2 is well supported by the transfer-function result (Fig. 8).
(8) The present conclusions concur with those of Harrison (1972), that the sources of sedimentation for the Purcell basin on the eastern and western sides were significantly different. One may also conjecture that those for the western side of the basin were quite rich in mineral content.

In several parts of the study area the conductors are present at shallow depths, making them viable drilling targets provided other sources of evidence, such as geochemical or structural interrelationships, indicate potential economic ore zones.

Fig. 14. The location of the MT survey lines in reference to the western Montana copper sulphide belt (patterned area) (note that only a few sites of Koocanusa (KOOC) lines 9 and 5 are near the eastern edge of the mined area). Some highly conducting areas in Fig. 11 are indicated by cross bars along the profile lines.

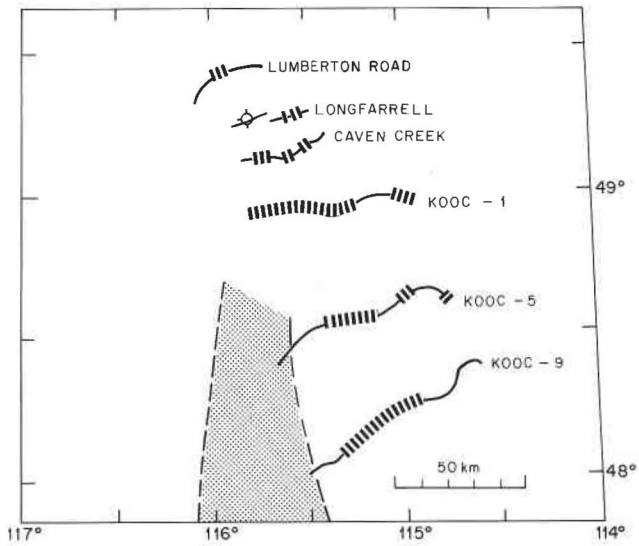

Acknowledgments

We wish to acknowledge Duncan Exploration Co. Ltd. (Denver, Colo.) for providing their MT data across the Purcell Anticlinorium in Canada, and Phoenix Geophysics Ltd. (Toronto) for permitting Lithoprobe access to their U.S. Koocanusa data at a low "academic" rate. Inversions were accomplished using Steve Constable and Catherine deGroot-Hedlin's Occam2 code as implemented in the Geotools© package, and a modified version of the Booker and Smith rapid relaxation inversion code provided by Torquil Smith. Torquil is thanked for the latter. We thank Jim Craven and Garry McNeice for extensive discussions during the analysis of these data; Drs. Dave Boerner, Ron Kurtz, and Yasuo Ogawa for their critical reviews of an early version of this paper; and Profs. Nigel Edwards and Ian Gough for their reviews of the submitted version.

References

Bally, A.W., Gordy, P.L., and Stewart, G.A. 1966. Structure, seismic data and orogenic evolution of Southern Canadian Rocky

Mountains. Bulletin of Canadian Petroleum Geology, **14**: 337–381.

Berdichevsky, M.M., and Dmitriev, V.L. 1976. Distortion of magnetic and electric fields by near surface lateral inhomogeneities. Acta geodaetica, geophysica et montanistica Hungarica, A Quarterly Journal of the Hungarian Academy of Sciences, **11**: 447–483.

Boberg, W.W. 1985. Geological and geophysical review of the results of the ARCO 1 Paul Gibbs well, Flathead County, Montana [abstract]. American Association of Petroleum Geologists Bulletin, **69**: 1042.

Clowes, R.M., Cook, F.A., Green, A.G., Keen, C.E., Ludden, J.N., Percival, J.A., Quinlan, G.M., and West, G.F. 1992. Lithoprobe: new perspectives on crustal evolution. Canadian Journal of Earth Sciences, **29**: 1813–1864.

Coney, P.J. 1989. Structural aspects of suspect terranes and accretionary tectonics in Western North America. Journal of Structural Geology, **11**: 107–125.

Coney, P.J., Jones, D.L., and Monger, J.W.H. 1980. Cordilleran suspect terranes. Nature (London), **288**: 329–333.

Constable, S.C., Parker, R.L., and Constable, C.G. 1987. Occam's inversion: a practical algorithm for generating models from electromagnetic sounding data. Geophysics, **52**: 289–300.

Cook, F.A., and Jones, A.G. 1995. Seismic reflections and electrical conductivity: a case of Holmes' curious dog? Geology, **23**: 141–144.

Cook, F.A., and Van der Velden, A. 1995. Three dimensional crustal structure of the Purcell Anticlinorium in the Cordillera of Southwestern Canada. Geological Society of America Bulletin, **107**: 642–664.

Cook, F.A., Green, A.G., Simony, P.S., Price, R.A., Parrish, R.R., Milkereit, B., Gordy, P.L., Brown, R.L., Coflin, K.C., and Patenaude, C. 1988. LITHOPROBE seismic reflection structure of the southeastern Canadian Cordillera: initial results. Tectonics, **7**: 157–180.

Craven, J.C., Jones, A.G., Boerner, D.E., Groom, R.W., and Kurtz, R.D. 1990. The correction of static shift in magnetotelluric data from the LITHOPROBE Southern Cordilleran transect. *In* Proceedings of the 60th Annual International Meeting of the Society of Exploration Geophysicists, San Francisco, 23–27 Sept. 1990. Extended abstracts, pp. 561–564.

deGroot-Hedlin, C. 1991. Removal of static shift in two dimensions by regularized inversion. Geophysics, **56**: 2102–2106.

deGroot-Hedlin, C., and Constable, S. 1990. Occam's inversion to generate smooth two-dimensional models from magnetotelluric data. Geophysics, **55**: 1613–1624.

Eisel, M., and Bahr, K. 1993. Electrical anisotropy in the lower crust of British Columbia: an interpretation of a magnetotelluric profile after tensor decomposition. Journal of Geomagnetism and Geoelectricity, **45**: 1115–1126.

Gough, D.I. 1986. Mantle upflow tectonics in the Canadian Cordillera. Journal of Geophysical Research, **91**: 1909–1919.

Gough, D.I., and Majorowicz, J.A. 1992. Magnetotelluric soundings, structure, and fluids in the southern Canadian Cordillera. Canadian Journal of Earth Sciences, **29**: 609–620.

Gough, D.I., Bingham, D.K., Ingham, M.R., and Alabi, A.O. 1982. Conductive structures in southwestern Canada: a regional magnetometer array study. Canadian Journal of Earth Sciences, **19**: 1680–1690.

Groom, R.W., and Bailey, R.C. 1989. Decomposition of magnetotelluric impedance tensor in the presence of local three-dimensional galvanic distortion. Journal of Geophysical Research, **94**: 1913–1925.

Groom, R.W., Kurtz, R.D., Jones, A.G., and Boerner, D.E. 1993. A quantitative methodology for determining the dimensionality of conductive structure from magnetotelluric data. Geophysical Journal International, **115**: 1095–1118.

Gupta, J.C., and Jones, A.G. 1990. Electrical resistivity structure of the Flathead Basin in southeastern British Columbia, Canada. Canadian Journal of Earth Sciences, **27**: 1061–1073.

Hamilton, J.M., Hauser, R., and Ransom, P. 1981. The Sullivan orebody. *In* Field guide to Geology and Mineral Deposits, Calgary '81, Annual Meeting, Geological Association of Canada, pp. 44–49.

Harrison, J.E. 1972. Precambrian Belt basin of northwestern United States: its geometry, sedimentation, and copper occurrences. Geological Society of America Bulletin, **83**: 1215–1240.

Harrison, J.E., Kleinkopf, M.D., and Obradovich, J.D. 1972. Tectonic events at the intersection of the Hope fault and Purcell trench, northern Idaho. United States Geological Survey, Professional Paper 719.

Hutton, V.R.S., Gough, D.I., Dawes, G.J.K., and Travassos, J. 1987. Magnetotelluric soundings in the Canadian Rocky Mountains. Geophysical Journal of the Royal Astronomical Society, **90**: 245–263.

Ingham, M.R. 1988. The use of invariant impedances in magnetotelluric interpretation. Geophysical Journal of the Royal Astronomical Society, **92**: 165–169.

Jones, A.G. 1986. Parkinsons' pointers' potential perfidy! Geophysical Journal of the Royal Astronomical Society, **89**: 1215–1224.

Jones, A.G. 1988. Static shift of magnetotelluric data and its removal in a sedimentary basin environment. Geophysics, **53**: 967–978.

Jones, A.G. 1992. Electrical conductivity of the continental lower crust. *In* Continental lower crust. *Edited by* D.M. Fountain, R.J. Arculus, and R.W. Kay. Elsevier Science Publishing Co., Inc., Amsterdam, pp. 81–143.

Jones, A.G., and Dumas, I. 1993. Electromagnetic images of a volcanic zone. Physics of the Earth and Planetary Interiors, **81**: 289–314.

Jones, A.G., and Groom, R.W. 1993. Strike angle determination from the magnetotelluric tensor in the presence of noise and local distortion: rotate at your peril! Geophysical Journal International, **113**: 524–534.

Jones, A.G., Kurtz, R.D., Oldenburg, D.W., Boerner, D.E., and Ellis, R. 1988. Magnetotelluric observations along the LITHOPROBE southern Canadian Cordilleran transect. Geophysical Research Letters, **15**: 677–680.

Jones, A.G., Kurtz, R.D., Boerner, D.E., Craven, J.A., McNeice, G.W., Gough, D.I., and DeLaurier, J.M. 1990. Electromagnetic investigation over the southern Cordilleran Lithoprobe Transect: 1991 status report. LITHOPROBE Cordilleran Workshop 1990, Extended Abstracts, pp. 64–74.

Jones, A.G., Kurtz, R.D., Boerner, D.E., Craven, J.A., McNeice, G.W., Gough, D.I., DeLaurier, J.M., and Ellis, R.E. 1991. Electromagnetic constraints on strike–slip fault geometry—the Fraser River fault system. Geology, **20**: 561–564.

Jones, A.G., Gough, D.I., Kurtz, R.D., DeLaurier, J.M., Boerner, D.E., Craven, J.A., Ellis, R.G., and McNeice, G.W. 1992. Electromagnetic images of regional structure in the southern Canadian Cordillera. Geophysical Research Letters, **12**: 2373–2376.

Jones, A.G., Groom, R.W., and Kurtz, R.D. 1993. Decomposition and modelling of the BC87 Dataset. Journal of Geomagnetism and Geoelectricity, **45**: 1127–1150.

Keller, G., Oltmans, J., and Passalacqua, H. 1990. Exploration of continental margin thrusted basins with deep electromagnetic sounding. *In* The potential of deep seismic profiling for hydrocarbon exploration. *Edited by* B. Pinet and C. Bois. Editions Technip, Paris, pp. 117–133.

Majorowicz, J.A., and Gough, D.I. 1991. Crustal structure from MT sounding in the Canadian Cordillera. Earth and Planetary

Science Letters, **102**: 444–454.

Marquis, G., Jones, A.G., and Hyndman, R.D. 1995. Coincident conductive and reflective lower crust across a thermal boundary in southern British Columbia, Canada. Geophysical Journal International, **120**: 111–131.

McNeice, G. 1994. Investigation of the Appalachians, Newfoundland, Canada. M.Sc. thesis, Department of Earth Sciences, Memorial University of Newfoundland, St. John's.

Monger, W.H., and Price, R.A. 1979. Geodynamic evolution of the Canadian Cordillera—progress and problems. Canadian Journal of Earth Sciences, **16**: 770–779.

Mozley, E.C., Goldstein, N.E., and Morrison, H.F. 1986. Magnetotelluric investigations at Mount Hood, Oregon. Journal of Geophysical Research, **91**: 11 596 – 11 610.

Parker, R.L. 1980. The inverse problem of electromagnetic induction: existence and constructions of solutions based on incomplete data. Journal of Geophysical Research, **85**: 4421–4428.

Parkinson, W.D. 1959. Direction of rapid geomagnetic fluctuations. Geophysical Journal of the Royal Astronomical Society, **2**: 1–14.

Parkinson, W.D. 1962. The influence of continents and oceans on geomagnetic variations. Geophysical Journal of the Royal Astronomical Society, **6**: 441–449.

Price, R.A. 1964. The Precambrian Purcell system in the Rocky Mountains of southern Alberta and British Columbia. Bulletin of Canadian Petroleum Geology, Guidebook, Special Issue No. 12, pp. 399–426.

Price, R.A. 1981. The cordilleran foreland thrust and fold belt in the southern Canadian Rocky Mountains. *In* Thrust and nappe tectonics. *Edited by* K.R. McClay and N.J. Price. Geological Society of London, Special Publication 9, pp. 427–448.

Ranganayaki, R.P. 1984. An interpretative analysis of magnetotelluric data. Geophysics, **49**: 1730–1748.

Schmucker, U. 1970. Anomalies of geomagnetic variations in the southwestern United States. Bulletin of the Scripps Institution of Oceanography No. 13.

Smith, J.T., and Booker, J.R. 1991. Rapid inversion of two and three dimensional magnetotelluric data. Journal of Geophysical Research, **96**: 3905–3922.

Sternberg, B.K., Washburne, J.C., and Pellerin, L. 1988. Correction for the static-shift in magnetotellurics using transient electromagnetic soundings. Geophysics, **53**: 1459–1468.

Sule, P.O., and Hutton, V.R.S. 1986. A broad-band magnetotelluric study in southeastern Scotland. Data acquisition, analysis and one-dimensional modelling. Annales Geophysicae, Series B, **4**: 145–156.

Wu, N., Booker, J.R., and Smith, J.T. 1993. Rapid two-dimensional inversion of COPROD2 data. Journal of Geomagnetism and Geoelectricity, **45**: 1073–1087.

Wynn, J.C., Kleinkopf, M.D., and Harrison, J.E. 1977. Audio-frequency magnetotelluric and gravity traverse across the crest of the Purcell anticlinorium, northwestern Montana. Geology, **5**: 309–312.

Yoos, T.R., Christopher, J.P., Thigpen, J.L., and Brown, L.D. 1991. The Cordilleran Foreland Thrust Belt in northwestern Montana and northern Idaho from COCORP and industry seismic reflection data. American Association of Petroleum Geologists Bulletin, **75**: 1089–1106.